(M_w 2.6) Delhi earthquakes, Bansal *et al.*[3] generated focal mechanism solutions based on the first motion and waveform modelling. Based on these solutions the authors suggested that these earthquakes involved normal faulting with a large strike–slip component. The focal mechanism of the Delhi earthquake of 25 November 2007 (M_w 4.1) computed by Singh *et al.*[4], shows strike–slip faulting with some normal component similar to the above-mentioned two small events in the area. On the contrary, Shukla *et al.*[6] reported thrust faulting with minor strike–slip component for small and regional earthquakes in and around Delhi. Since the focal mechanism reported by them is not well constrained, a comparison may not be appropriate.

- The strong ground-motion histories recorded by the local array of accelerographs will be of immense help in developing hazard scenarios due to future earthquakes in the region. This is an important step in the preparation of specific modules for mitigating the risk due to such events.
- Although there is general awareness of the seismic hazard that Delhi is exposed to, the current scientific knowledge and data need to be improved.

1. IS: 1893 Part-I, Indian standard criteria for earthquake resistant design of structures. Part 1, general provisions and buildings (fifth revision). Bureau of Indian Standards, New Delhi, 2002, p. 42.
2. Verma, R. K. *et al.*, Seismicity of Delhi and the surrounding region. *J. Himalayan Geol.*, 1995, **6**, 75–82.
3. Bansal, B. K., Singh, S. K., Dharmaraju, R., Pacheco, J. F., Ordaz, M., Dattatrayam, R. S. and Suresh, G., Source study of two small earthquakes of Delhi, India, and estimation of ground motion from future moderate, local events. *J. Seismol.*, 2009, **13**, 89–105.
4. Singh, S. K. *et al.*, Delhi earthquake of 25 November 2007 (M_w 4.1): implications for seismic hazard. *Curr. Sci.*, 2010, **99**, 939–947.
5. Chandra, U., Seismicity, earthquake mechanisms and tectonics along the Himalayan mountain range and vicinity. *Phys. Earth Planet. Inter.*, 1978, **16**, 109–131.
6. Shukla, A. K., Prakash, R., Singh, R. K., Mishra, P. S. and Bhatnagar, A. K., Seismotectonics implications of Delhi region through fault plane solutions of some recent earthquakes. *Curr. Sci.*, 2007, **93**, 1848–1853.

ACKNOWLEDGEMENTS. We thank the Secretary, Ministry of Earth Sciences, Government of India for support and encouragement. We also thank IMD, IIT-Roorkee (Dr Ashok Kumar and his team) and other organizations which operate and maintain the seismic stations in the country. R. S. Dattrayam provided the preliminary report of the earthquake and G. Suresh computed the final epicentre. We also thank Dr K. Rajendran for reviewing the paper.

Received 6 May 2012; accepted 14 May 2012

Impact of population density on the surface temperature and micro-climate of Delhi

Javed Mallick[1] and Atiqur Rahman[2,*]

[1]Department of Civil Engineering, King Khalid University, Abha, Kingdom of Saudi Arabia
[2]Remote Sensing and GIS Division, Department of Geography, Faculty of Natural Sciences, Jamia Millia Islamia University, New Delhi 110 025, India

Increasing urban surface temperature due to change of natural surfaces is one of the growing environmental problems in urban areas, especially in cities like Delhi. The present work is an attempt to assess the urban surface temperature in Delhi using remote sensing and GIS techniques. ASTER datasets of thermal bands were used to assess the land surface temperature (LST) using temperature emissivity separation technique. Ward-wise population density was calculated from the Census of India 2001 data to correlate the population density with LST. The study shows that surface temperature changes with the increase in the impervious surface area, which is related to the increase in the population density.

Keywords: Micro-climate thermal bands, population density, surface temperature, thermal bands.

IN today's world of globalization and industrialization, urban environmental studies have become an important area of research. Land surface temperature (LST) is a critical parameter in urban climatology[1]. Remote sensing satellite data have been utilized to assess urban land surface thermal characteristics through mapping and assessing surface temperature from thermal infrared images[2]. In the urbanization process (demographic pressure), removal of natural land-cover types and their replacement with common urban materials such as concrete, asphalt, stone, brick and metal has significant effect on the environment, including reduction in evapotranspiration, promotion of more rapid surface run-off, increased storage and transfer of heat that can be sensed, and deterioration of air and water quality. The result of this change can have significant effects on local weather and climate[3]. Substantial amount of the variance of temperature rise in cities is explained as a function of population growth[4]. The holistic impacts of land surface cover, water and vegetation discussed above have climatological and meteorological implications on the urban atmosphere at various scales and all of these factors are linked with population growth. There is little doubt that population growth impacts local climate[5–12]. Micro-climate change intensity [as change in urban heat island (UHI) intensity] tends to increase with increasing city size and/or population[13–20], and as cities

*For correspondence. (e-mail: ateeqgeog@yahoo.co.in)

grow, they increasingly contribute to climate change at scales beyond the local. For North American and European cities, Oke[21] developed a regression model that successfully explained that 97% of the variability in UHI intensity is due to a single predictor variable – the population size. An analysis of urban temperature changes in USA based on population showed a local increase of approximately 1°C per 100,000 people due to urbanization[22]. The effects of urbanization on climate change have been analysed using meteorological and population data of urban and rural areas[22] and measurements of LST using night-light satellite data[23,24]. The climate in and around cities and other built-up areas is altered due to changes in land-use/land-cover (LU/LC) and anthropogenic activities related to urbanization[2].

In interpretation and analysis of thermal satellite images for temperature distribution over complex areas, one looks for patterns of relative temperature differences, rather than the absolute values. This is because many complex factors make quantitative determinations difficult, such as number and distribution of different material classes in an instantaneous field of view (IFOV). Spectral thermal response is dependent on composition, density and texture of the materials; vegetation canopy characteristics, including height, leaf geometry and plant shape and near-surface (1–3 m) air temperature; relative humidity and wind effects[25]. This thermal behaviour of urban surfaces over a certain period of time would yield a good database for urban planners and architects for improving city site quality by making it more eco-friendly. This would be particularly beneficial to India and some other countries with tropical to subtropical climate.

Metropolitan areas like Delhi are the main engines of urban growth in India[26]. Rapid and haphazard urban growth and accompanying population pressures, result in changes in urban LU/LC; loss of productive agricultural land and open green spaces; loss of surface water bodies; depletion of groundwater; micro-climate change and air, water and noise pollution[27]. Delhi has witnessed a phenomenal population growth during the past few decades. According to the Census of India 2001 figures, Delhi's population was only 0.4 million in 1901; it increased to 13.8 million in 2001 and to 16.75 million in 2011. The process of urbanization in Delhi in terms of net growth of population has been faster in the recent decade (20.96% during 2001–2011). This coupled with changes in economic activities has resulted in changes in the socio-economic structure of the population and also changes in the urban environment, including LST. In this study the night-time ASTER thermal bands have been processed to obtain LST to study the UHI effect associated with population density in Delhi Metropolitan City. The data used in this study are as follows:

- ASTER satellite data of 7 October 2001 (night-time), path/row – 13/204, five thermal bands, i.e. 10–14 (8.125–11.65 μm), 90 m spatial resolution.
- Ward-wise boundary map of Delhi as a geodatabase.
- Ward-wise population data for Delhi according to the Census of India 2001.

Delhi is situated between 28°23′17″–28°53′00″N lat. and 76°50′24″–77°20′37″E long. It lies at an altitude between 213 and 305 m amsl and covers an area of 1483 sq. km. It is situated mainly on the west bank of the River Yamuna. The city is bordered in the east by Uttar Pradesh and in the north, west and south by Haryana. The climate of Delhi is influenced by its remote inland position and prevalence of air of continental character, which is characterized by extreme summer heat in June (48°C), alternating with severe winter cold in December (3°C). Rainfall is recorded mainly during the monsoon months of July–September.

Population density was calculated from the Census of India 2001 data and it has been divided into five classes, from very low to very high density. Figure 1 and Table 1 show that only two wards in the oldest part of Delhi, namely ward 19 (Darya Ganj) and ward 107 (Bazar Sitaram) have very high population density (90,001–225,993). The high-density wards are mainly in the eastern and central parts of Delhi, whereas the very low population density wards are in the suburbs of the city, located in the northern, southern and western part of

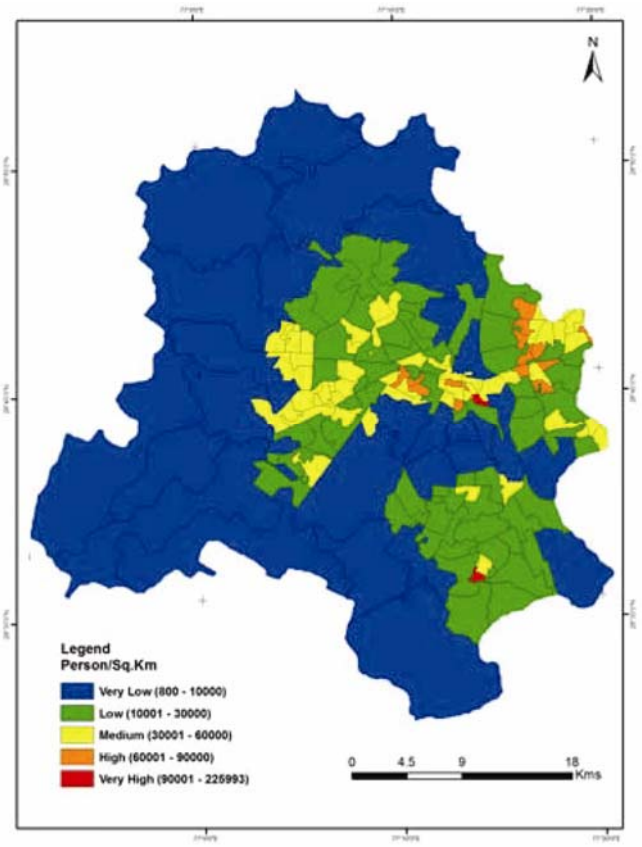

Figure 1. Population density of Delhi in 2001.

Table 1. Ward-wise population density of Delhi (2001)

Population density	Range	Ward number
Very low	800–10,000	50, 37, 102, 58, 55, 53, 101, 1000, 10003, 104, 10005, 44, 56, 10004, 38, 10001, 49, 127, 36, 10009, 48, 2, 57, 65, 114, 116 and 67
Low	10,001–30,000	12, 59, 14, 94, 115, 71, 63, 34, 7, 60, 4, 30, 10006, 79, 100, 13, 129, 106, 80, 66, 8, 5, 16, 15, 9, 118, 91, 97, 27, 19, 64, 123, 18, 1, 10007, 103, 33, 32, 54, 10008, 26, 119, 68, 69, 82, 17, 51, 23, 74, 117, 99, 11, 10002, 87, 133, 35, 124, 10 and 73
Medium	30,001–60,000	31, 43, 83, 46, 22, 72, 47, 125, 25, 20, 6, 110, 3, 126, 28, 70, 40, 122, 29, 120, 77, 41, 128, 42, 39, 86, 105, 132, 113, 52, 90, 75, 24, 45, 85, 96, 111, 121, 21, 62, 88 and 131
High	60,001–90,000	134, 95, 78, 130, 76, 84, 89, 98, 93, 92, 112, 108, 81 and 61
Very high	90,001–25,993	109 and 107

Delhi. These latter areas were formerly agricultural lands and are still being converted into residential land. Therefore, these wards have less population density.

In this study, an attempt has also been made to measure the surface emissivity using the emissivity box[28]. All the measurements of temperature were done using TELATEMP infrared radiometer which operates in the 8–14 μm waveband with an IFOV of 2°C and accuracy of 0.1°C. The measurements were made during 4–6 October 2005 at various places taking different features of interest on all sunny days at different hours of the day. This is achieved in the field by exposing the hot lid to direct solar radiation for 15 min so that thermal equilibrium can be attained. To reduce the effect of noise in the final result, the value is taken after averaging over 10–15 successive measurements. The emissivity values presented here are the results of *in situ* measurements in and around Delhi. The measurements could not be made on all the sample features in the area, but were only carried out over some selected (dominant) features representing that LU/LC class. The measurements were carried out on soil (for wasteland/bare soil), dense vegetation, sparse vegetation, agricultural crops and urban (concrete, asphalt roads and sandstone) segments. To determine the sample emissivity, the hot lid temperature must be higher than the sample temperature (15–20°C) and remain constant during the time necessary for making L^1 and L^2 measurements. The emissivity measurement was rapidly made (within 2 min) in order that the temperature variation of the hot lid can be negligible when it is introduced in the box. The emissivity measurement was carried out during the middle of the sunny day when the stability of the system is greater. The emissivity values measured for soil and vegetation by the box method using the radiometer are shown in Table 2. It can be seen that there is not much variation in emissivity values either throughout the day or between the clear days of the period. Hence, the average of the measurements can be taken as the values of the respective samples. The mean can be considered as a representative value that can be used in practice, whereas standard deviations show the variability in emissivity values. The measured emissivity values were compared with those measured by Owe and Griend[29].

Gillespie *et al.*[30] proposed a new temperature emissivity separation (TES) technique for Terra ASTER data. TES attempts to compensate for reflected down-welling irradiance and estimates the absolute spectral emissivity. The additional constraint to overcome under-estimation comes from the regression of the minimum emissivity of spectral contrast (calculated from laboratory spectra), which is used to equalize the number of unknowns and measurements. ASTER has 14 spectral bands, out of which five thermal bands (10–14) operate between 8 and 12 μm. In this study, using the TES algorithm five emissivity maps and one surface temperature map were produced. It not only estimates the temperature of homogeneous areas of known emissivity, such as water bodies, but also for heterogeneous areas of unknown emissivity.

Figure 2 shows the night-time surface temperature derived from ASTER data of 7 October 2001 at 22 : 35 h. (local time).

The study shows that the estimated surface temperature ranges from 23.90°C to 40.01°C (mean value, 31.40°C and standard deviation, 1.863). It has been observed that the central and eastern parts of the study area, i.e. Chandni Chowk, Mangolpuri, Uttam Nagar, Okhla Phase I, Shahdara, Lakshminagar, Mayapuri Industrial Area and Narela Industrial Area have maximum surface temperature (34°C–40°C). These areas dominated by commercial activities have low vegetation cover and high population density with impervious surface. The medium surface temperature (30°C–34°C) has been recorded in the suburbs where there are less built-up areas, e.g. Dhaula Kuan, Uttam Nagar, Pusa Institute, IGI Airport and Akbarpur.

Lower night-time surface temperatures (24°C–30°C) are seen in the north, north-west, south and towards the eastern part of River Yamuna. These areas have dense vegetation, fallow land and scrubs/bare soil, which

Table 2. Field measurements of emissivity in the 8–14 μm bands for different samples

Date	Soil	Sparse vegetation	Dense vegetation	Urban (concrete)	Agricultural cropland (Paddy)
4 October 2005	0.923 ± 0.013	0.9560 ± 0.015	–	0.9156 ± 0.012	–
5 October 2005	–	–	0.9810 ± 0.006	–	0.9850 ± 0.013
6 October 2005	–	0.9775 ± 0.016	0.9807 ± 0.012	0.9378 ± 0.014	–
Mean	0.923 ± 0.013	0.9668 ± 0.015	0.9808 ± 0.09	0.9267 ± 0.013	0.9850 ± 0.013

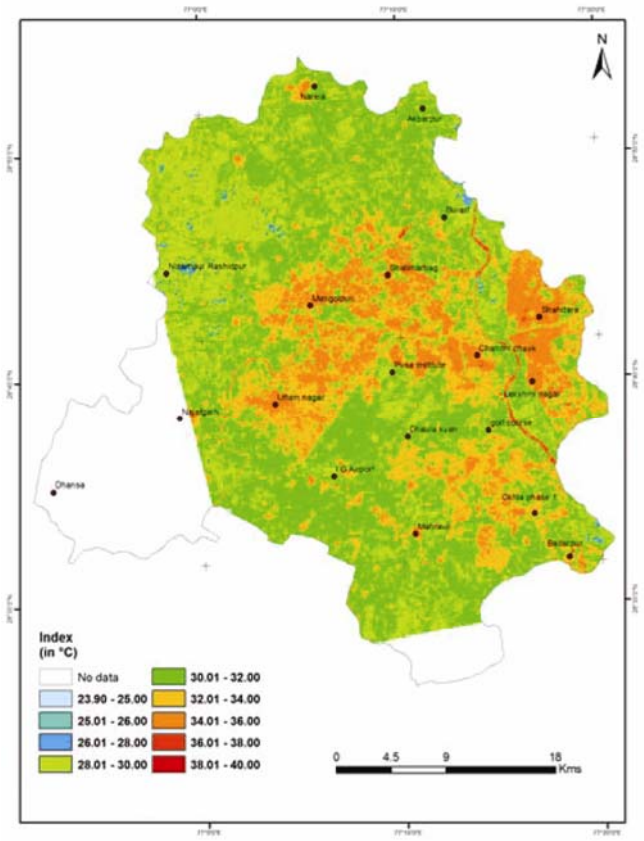

Figure 2. Night-time land surface temperature of Delhi derived from ASTER data of 7 October 2001.

remain cooler during night-time compared to other areas where land has been developed for urban land use. It was also seen that the thermal gradient increases from built-up area (centre of Delhi) to non built-up area (north and south of Delhi). When compared with daytime surface temperature, it has been observed that over the water bodies, the highest surface temperature varies between 36°C and 40°C in the northeast to southeast of the study area. This may be because water bodies cool slowly during the night-time due to high thermal inertia, convection, wave action and turbulence.

A close examination of the night-time surface temperature map shows that there is a gradual thermal change from the Central Business District (CBD) into the suburbs of the city. The city centre has less vegetation and some hotspots can be seen over the built-up area accounting for higher surface temperature than in the outskirts.

The surface temperature for 2001 was measured using satellite data and the field survey was conducted in 2005. In this situation it was assumed that surface features observed on the ground in 2005 were the same in 2001. Three natural surfaces in this dense vegetation such as tree cover, green grass and bare soil and two artificial surfaces (two different roofs inside the city where fixed points of measurement were assembled) were selected. Vegetation samples were measured for suites of plant materials such as green leaves. The average temperature in the area covered with vegetation was 29.7°C using field measurement and it was 31.02°C as derived from satellite imagery data. In contrast, on concrete urban surface, field observation showed a temperature of 30.10°C and satellite imagery data yielded a temperature of 31.46°C. The discrepancy between the values from the two methods of measurement of surface temperature is within the range ± 1.5°C. Despite this difference, it can be concluded that the temperature estimates by the two methods are roughly similar[31].

A relationship has been drawn between night-time surface temperature of 2001 and population density of 2001. Night-time surface temperature of Delhi in 2001 estimated from thermal satellite data has been clubbed into three surface temperature groups, i.e. low, medium and high, whereas the ward-wise population density data of 2001 taken from the Census of India have been classified into five groups from very low to very high (represented in the map by proportional solid circles). These two spatial data layers were superposed using ArcGIS software (Figure 3). This has been done in order to study the role of population density as one of the major factors for increasing the surface temperature of the city.

Figure 3 shows high-surface temperature in the east, southeast and central parts of the city that correspond to densely built-up area. These densely built-up areas are mainly because of increased economic activity and the fast development of residential societies to provide housing to the increasing population. The increase in population density in turn leads to higher surface temperature in these particular areas. Figure 3 clearly shows that the areas of high and very high population density also have high surface temperature.

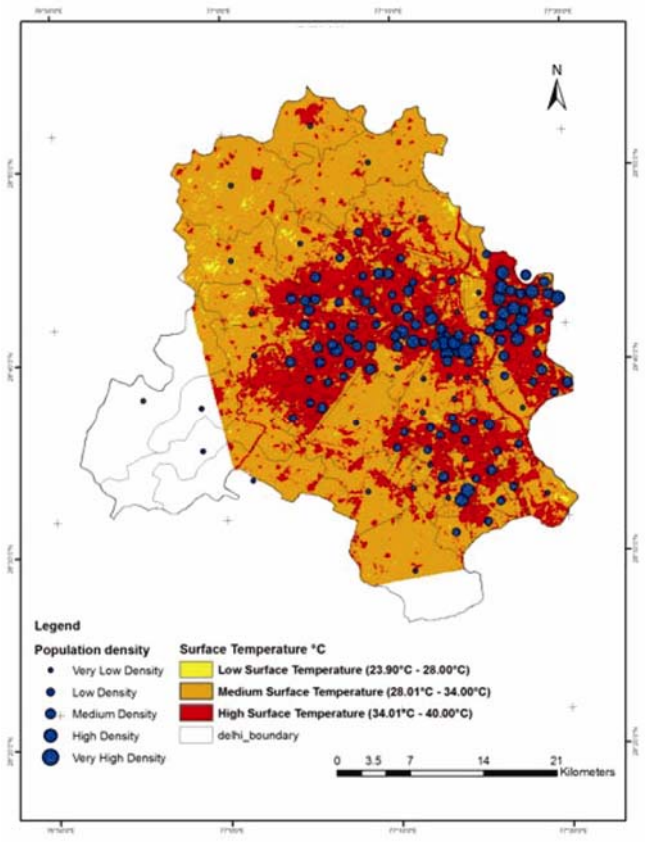

Figure 3. Relationship between night-time surface temperature and population density in Delhi in 2001.

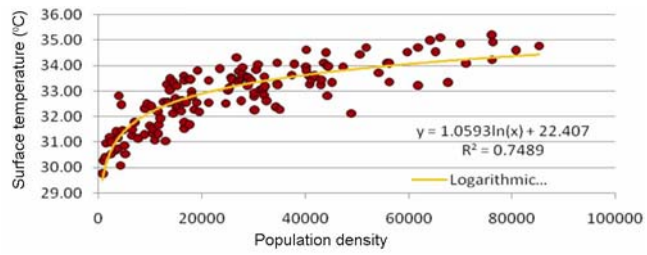

Figure 4. Correlation between night-time surface temperature and population density.

Figure 4 shows the correlation between surface temperature and population density. A strong positive correlation between the two can be seen. The value of logarithmic regression (R^2) is 0.748. The logarithmic regression equation between surface temperature and population density is $Y = 1.059\ln \times \text{Pop-density} + 22.40$. It means that with the increase in population density, surface temperature also increases. Furthermore, it is possible to predict night-time surface temperature on the basis of known population density.

The substantial amount of variance of temperature rise in cities could be explained as a function of population growth. The growing cities showed the highest warming rates and square root of the population number as the most representative factors for the urban contribution to temperature change[4]. Oke[21] used the empirical method to represent the relationship between urban–rural temperatures as concentration on population. It is not easy to separate many contributors to the problem. However, one of the most noticeable and one that has proven to have an extremely strong correlation with the UHI phenomenon or urban surface temperature is the population density of major cities[32]. The present study demonstrates a close relationship between the population density, built-up area and surface temperature. The statistical analysis of night-time surface temperature with population density indicates that population growth tends to contribute to the urban surface temperature rise or UHI intensity and also to the micro-climate of Delhi.

In earlier times and even now, there are very few meteorological stations to record the surface temperature, and they may not be the true representative for the whole city. In such situations, LST derived from thermal satellite data are useful to study the variation of surface temperature over the entire city area that is an important parameter for micro-climate of urban areas. This study clearly shows spatial variation of LST over entire Delhi. By superposing the population density map of Delhi over the surface temperature map, it can be clearly seen that high population density is one of the main contributing factors for the high surface temperature, UHI intensity and also micro-climate of Delhi. To assess and address the issue of micro-climate and also to mitigate the impact of UHI on the city population, the outcome of such types of studies may be useful.

1. Voogt, J. A. and Oke, T. R., Thermal remote sensing of urban climates. *Remote Sensing Environ*., 2003, **86**, 370–384.
2. Mallick, J., Rahman, A., Hoa, P. V. and Joshi, P. K., Assessment of night-time urban surface-temperature land use/cover relationship for thermal urban environment studies using optical and thermal satellite data. In TS 1G – Remote Sensing for Sustainable Development, 7th FIG Regional Conference Spatial Data Serving People: Land Governance and the Environment – Building the Capacity Hanoi, Vietnam, 19–22 October 2009.
3. Landsberg, H. E., *The Urban Climate*, New York, Academic Press, 1981.
4. Mitchell, J. M., The temperature of cities. *Weather-wise*, 1961, **14**, 224–229.
5. Tso, C. P., A survey of urban heat island studies in two tropical cities. *Atmos. Environ.*, 2001, **30**, 507–519.
6. Jauregui, E., Heat island development in Mexico City. *Atmos. Environ*., 1997, **31**, 3821–3831.
7. Tayanc, M. and Toros, H., Urbanization effects on regional climate change in the case of four large cities of Turkey. *Climate Change*, 1997, **6**, 59–69.
8. Brandsma, T., Können, G. P. and Wessels, H. R. A., Emperical estimation of the effect of urban heat advection on the temperature series of De Bilt (The Netherlands). *Int. J. Climatol*., 2003, **23**, 829–845.
9. Chung, U., Choi, J. and Yun, J. I., Urbanization effect on the observed change in mean monthly temperatures between 1951–1980 and 1971–2000 in Korea. *Climatic Change*, 2004, **66**, 127–136.
10. Mihalakakou, G., Santamouris, M., Papanikolaou, N., Cartalis, C. and Tsangrassoulis, A., Simulation of the urban heat island pheno-

menon in Mediterranean climates. *Pure Appl. Geophys.*, 2004, **161**, 429–451.
11. Stallings, J. A., Characteristics of urban lightning hazards for Atlanta, Georgia. *Climatic Change*, 2004, **66**, 137–150.
12. Zhou, L. M. *et al.*, Evidence for a significant urbanization effect on climate in China. *Proc. Natl. Acad. Sci. USA*, 2004, **101**, 9540–9544.
13. Park, H. S., Features of the heat island in Seoul and its surrounding cities. *Atmos. Environ.*, 1986, **20**, 1859–1866.
14. Yamashita, S., Sekine, K., Shoda, M., Yamashita, K. and Hara, Y., On relationships between heat island and sky view factor in the cities of Tama River basin, Japan. *Atmos. Environ.*, 1986, **20**, 681–686.
15. Chow, S. D., The urban climate of Shanghai. *Atmos. Environ., Part B, Urban Atmos.*, 1992, **26**, 9–15.
16. Hogan, A. W. and Ferrick, M. G., Observations in nonurban heat islands. *J. Appl. Meteorol.*, 1998, **37**, 232–236.
17. Magee, N., Curtis, J. and Wendler, G., The urban heat island effect at Fairbanks, Alaska. *Theor. Appl. Climatol*., 1999, **64**, 39–47.
18. Philandras, C. M., Metaxas, D. A. and Nastos, P. T., Climate variability and urbanization in Athens. *Theor. Appl. Climatol.*, 1999, **63**, 65–72.
19. Torok, S. J., Morris, C. J. G., Skinner, C. and Plummer, N., Urban heat island features of southeast Australian towns. *Aust. Meteorol. Mag.*, 2001, **50**, 1–13.
20. Hinkel, K. M., Nelson, F. E., Klene, A. F. and Bell, J. H., The urban heat island in winter at Barrow, Alaska. *Int. J. Climatol*., 2003, **23**, 1889–1905.
21. Oke, T. R., City size and the urban heat island. *Atmos. Environ*., 1973, **7**, 769–779.
22. Karl, T. R., Diaz, H. F. and Kukla, G., Urbanization: its detection and effect in the United States climate record. *J. Climate*, 1998, **11**, 1099–1123.
23. Gallo, K. P., Tarpley, J. D., McNab, A. L. and Karl, T. R., Assessment of urban heat islands: a satellite perspective. *Atmos. Res.*, 1995, **37**, 37–43.
24. Peterson, T. C., Gallo, K. P., Lawrimore, J., Owen, T. W., Huang, A. and McKittrick, D. A., Global rural temperature trends. *Geophys. Res. Lett*., 1999, **26**, 329–332.
25. Short, N. M., *The Remote Sensing Tutorial*, Goddard Space Flight Centre, NASA, USA, 2010.
26. Rahman, A., Netzband, M., Singh, A. and Mallick, J., An assessment of urban environmental issues using remote sensing and GIS techniques an integrated approach: a case study: Delhi, India. In *Urban Population – Environment Dynamics in the Developing World: Case Studies a Lessons Learned* (eds De Sherbinin, A. *et al.*), International Cooperation in National Research in Demography, Paris, 2009, pp. 181–211.
27. Rahman, A., Application of remote sensing and GIS technique for urban environmental management and sustainable development of Delhi, India. In *Applied Remote Sensing for Urban Planning, Governance and Sustainability* (eds Netzband, M., Stefnow, W. L. and Redman, C. L.), Springer-Verlag, Berlin, 2007, pp. 165–197.
28. Kant, Y. and Badarinath, K. V. S., Ground based method for measuring thermal infrared effective emissivities: implications and perspectives on the measurement of land surface temperature from satellite data. *Int. J. Remote Sensing*, 2002, **23**, 2179–2191.
29. Owe, M. and Griend, Van de, Ground based measurement on surface temperature and thermal emissivity. *Adv. Space Res.*, 1994, **14**, 45–58.
30. Gillespie, A., Rokugawa, S., Matsunaga, T., Steven Cothern, J., Hook, S. and Kahle, A. B., A temperature and emissivity separation algorithm for Advanced Space borne Thermal Emission and Reflection Radiometer (ASTER) images. *IEEE Trans. Geosci. Remote Sensing*, 1998, **36**, 1113–1126.
31. Caselles, V., Coll, C. and Valor, E., Land surface emissivity and temperature determination in the whole HAPEX – Sahel area from AVHRR data. *Int. J. Remote Sensing*, 1997, **18**, 1009–1027.
32. Lo, C. P. and Faber, B. J., Integration of landsat thematic mapper and census data for quality of life assessment. *Remote Sensing Environ.*, 1997, **62**, 143–157.

Received 5 November 2010; revised accepted 17 May 2012